

# Modeling Human Driving Behavior in Highway Scenario using Inverse Reinforcement Learning

Zhiyu Huang, Chen Lv, *Senior Member, IEEE*, Jingda Wu

**Abstract**—Human driving behavior modeling is of great importance for designing safe, smart, smooth as well as personalized autonomous driving systems. In this paper, an internal reward function-based driving model that emulates the human’s internal decision-making mechanism is proposed. Besides, a sampling-based inverse reinforcement learning (IRL) algorithm that learns the reward function from human naturalistic driving data is also developed. A polynomial trajectory sampler is adopted to generate feasible trajectories and approximate the partition function in the maximum entropy IRL framework, and a dynamic and interactive environment is built upon the static driving dataset to estimate the generated trajectories considering the mutual dependency of agents’ actions. The proposed method is applied to learn personalized reward functions for individual human drivers from the NGSIM dataset. The qualitative results demonstrate that the learned reward function is able to interpret their decisions. The quantitative results also reveal that the personalized modeling method significantly outperforms the general modeling approach, reducing the errors in human likeness by 24%, and the proposed reward-function-based method delivers better results compared to other baseline methods. Moreover, it is found that estimating the response actions of surrounding vehicles plays an integral role in estimating the trajectory accurately and achieving a better generalization ability.

**Index Terms**—Driving behavior modeling, inverse reinforcement learning, trajectory sampling, interaction awareness.

## I. INTRODUCTION

**H**UMAN-LIKE driving is an essential objective for autonomous vehicles (AVs) targeting widespread deployment in the real world. It is conceivable that AVs and human drivers share the road in the near future, which requires AVs to act like humans, thus being predictable and interpretable to other human drivers, in order to operate safely among humans. However, current autonomous driving systems fail to show such characteristics, which leads to conservative and unnatural decisions that confuse and even endanger other human drivers [1]. This is due to their inability to interact with other human traffic participants, more specifically, to reason about the surrounding agents’ possible behaviors and make proactive decisions accordingly. So as to address such a problem and enable a safe and efficient autonomous driving system, we need to model how human drivers behave in the presence of other road users. Understanding human driving behavior can enlighten the AV to reason about other agents’

intents or desires and informs the planning and decision-making process. Moreover, fitting the decision-making system to the expected driving style of a human user by modeling his or her preference for driving behavior can help achieve personalized driving experience [2].

Driving behavior modeling usually relates to motion prediction task [3], and most of the existing methods are performed at the phenomenon level, i.e., inferring the driver’s behavior based on current and historical observations. These includes parametric models such as the intelligent driver model (IDM) [4] and minimizing overall braking induced by lane changes (MOBIL) model [5], and neural network models such as long short-term memory (LSTM) network [6], convolutional neural network (CNN) [7], and graph neural network (GNN) [8]. The internal reward-based method, on the other hand, formulates the motivation of agents choosing actions and is believed to better reflect the human’s internal decision-making scheme. It presumes that humans are rational drivers who choose the actions that optimize their internal reward (or equivalently negative cost) functions, and the internal reward can encode not only the basic requirements for driving safely but also the preference of a human driver. Moreover, the internal reward model is succinct and highly interpretable because of its explicit physical meanings [9] and more data-efficient and computationally-efficient due to a small number of parameters to learn. For personalized driving, the learned reward function can be incorporated into the planning module of an AV to fit the preference of the human user. For predicting the motion of other vehicles, some planning methods (e.g., game theory and trajectory optimization) can be used if the internal reward functions of other drivers are obtained [10].

In order to infer the internal reward functions of human drivers, inverse reinforcement learning (IRL) has emerged as the main approach to learn the parameters of reward function from human demonstrations. Given a set of trajectories of human driving in a scenario, IRL attempts to recover the underlying reward function of the agent that best describes the human demonstrations. The core idea is to adjust the weights of the reward function to yield a policy that matches the demonstration trajectories. Recently, maximum entropy IRL [11] has seen extensive use in modeling real-world driving behaviors [12]–[16], thanks to its capability in addressing the stochasticity of human driving behavior and the ambiguity that many reward functions could result in the same trajectory. The maximum entropy IRL states that expert behavior follows a distribution over trajectories and the probability of a trajectory is exponential to the reward of the trajectory. However, in the autonomous driving domain, continuous and large-scale state

Z. Huang, C. Lv and J. Wu are with the School of Mechanical and Aerospace Engineering, Nanyang Technological University, Singapore, 639798. (e-mail: zhiyu001@e.ntu.edu.sg, lyuchen@ntu.edu.sg, jingda001@e.ntu.edu.sg)

This work was supported by the SUG-NAP Grant (No. M4082268.050) of Nanyang Technological University, Singapore.

Corresponding author: C. Lv

and action spaces pose a daunting challenge to the maximum entropy IRL algorithm, essentially due to the intractability of calculation of the partition function involving all possible trajectories.

In light of this, numerous studies have proposed their solutions to approximate the partition function. [12], [13] use Laplace approximation to reshape the reward function of a trajectory considering only local optimal [17], enabling the partition function to be solved analytically. This makes continuous states and actions tractable in the IRL algorithm, but the assumption of local optimal may not stand in real-world cases. For the autonomous driving domain, we can make some convenient assumptions with domain knowledge to enable the IRL algorithm easier to solve. One way is to assume that a human driver is an optimizer that only follows the optimal actions with respect to the internal reward function, and thereby only the optimal trajectory is considered as the feasible trajectory. [14], [15] propose to generate the optimal trajectory by minimizing the updated reward function and calculate the feature expectation on the optimal trajectory. [18] utilizes a spatiotemporal state lattice planner to find an optimal trajectory for calculating feature expectation in the IRL framework. Another way is to assume that a human driver can create multiple candidate trajectories in mind and select one to execute according to their associated rewards. This assumption is intuitive and well explains the stochasticity of human driving behavior, and the generated trajectories can serve as the feasible trajectories in the partition function. [16] suggests generating feasible trajectory samples with elastic band path planning and speed profile sampler to estimate the partition function and further the feature expectation in the IRL algorithm, which demonstrates better modeling accuracy than the Laplace approximation and optimal trajectory methods. It has been demonstrated that the sampling-based approximation method is more apt in the framework of maximum entropy IRL, and the sampling-based IRL method has shown its potential in tuning the reward function of the trajectory planner online to match human driving styles [19], [20].

However, the main limitation of previous studies is the assumption that all vehicles in the human driving dataset share one common cost function, which certainly violates the fact that human driving behaviors are diverse and personalized. Furthermore, the mutual dependency of the ego vehicle's and other vehicles' actions is not considered due to the static dataset, which hardly reflects the interactions between humans in the real-world driving scenarios. For example, if the ego vehicle were attempting a lane-change which not exists in the original dataset, the influenced vehicle on that lane should decelerate to yield rather than crash into the ego vehicle per the fixed trajectory. We demonstrate that simulating such responsive actions is important for the sampling-based IRL method to estimate the reward of the generated trajectory in a close-to-human way. Moreover, by simulating how humans may respond to the ego vehicle's actions, we can incorporate the interaction awareness, represented by the other vehicles' travel efficiency loss induced by the ego vehicle's behavior, into the cost function, which helps better explain the human driving behavior, as supported by previous works [21], [22].

In this paper, we use the sampling-based IRL method to learn diverse and mixed cost functions of different human drivers considering highly interactive driving behaviors from a naturalistic highway driving dataset. The interactive feature is achieved by building a dynamic and interactive environment based on real-world human driving data. The environment populates the ego vehicle and surrounding vehicles with interactive behaviors beyond the fixed trajectories in the dataset (e.g., other vehicles can yield to the ego vehicle and avoid collision with it), to generate ensemble trajectories in the driving scene, which represent mutual influence between agents. The main contributions of this paper are listed as follows.

- 1) A sampling-based inverse reinforcement learning algorithm integrating polynomial curve trajectory sampler is proposed. Besides, a highly interactive environment built upon real-world human driving data is used to simulate the possible vehicle interactions under the sampled trajectories.
- 2) Two modeling assumptions, which are personalized modeling (each driver possesses a distinct cost function) and general modeling (all drivers share a common cost function), are investigated. The personalized modeling method shows superiority over the general modeling method in terms of modeling accuracy.
- 3) The effects of the simulated interactive behaviors and the agent's interaction awareness are investigated. The results indicate that the two factors are of importance in estimating the reward of the generated trajectory and expressing the interactions in human driving behaviors.

In the remainder of this paper, Section II formulates the problem of driving behavior modeling mathematically and introduces the maximum entropy IRL with trajectory sampling. Section III details the human driving dataset, the interactive driving environment, the selection of driving features, and the settings of the experiments. Section IV displays the results of the learning process and interpretation of human driving behavior, compares the modeling accuracy of different modelling methods, and analyzes the effects of interaction factors. Finally, conclusions are summarized in Section V.

## II. METHODOLOGY

The proposed framework for human driving behavior modeling is illustrated in Fig. 1. We assume that the human driving behavior consists of three processes, namely trajectory generation, trajectory evaluation, and trajectory selection. Given a driving scenario, a human driver first creates multiple candidate trajectories in mind, which relate to high-level decisions (e.g., lane change and lane-keeping) and speed requirements. At the same time, the driver should anticipate the results of the trajectories (involving interactive and risk-averse behaviors) and evaluate the rewards of different trajectories (involving personal preference). The potential plans are assigned with probabilities according to the Boltzmann noisily-rational model (soft-max), and the trajectory with the highest probability is then selected and finally executed. This assumption makes it justifiable for the proposed sampling-based inverse reinforcement learning algorithm, which is used

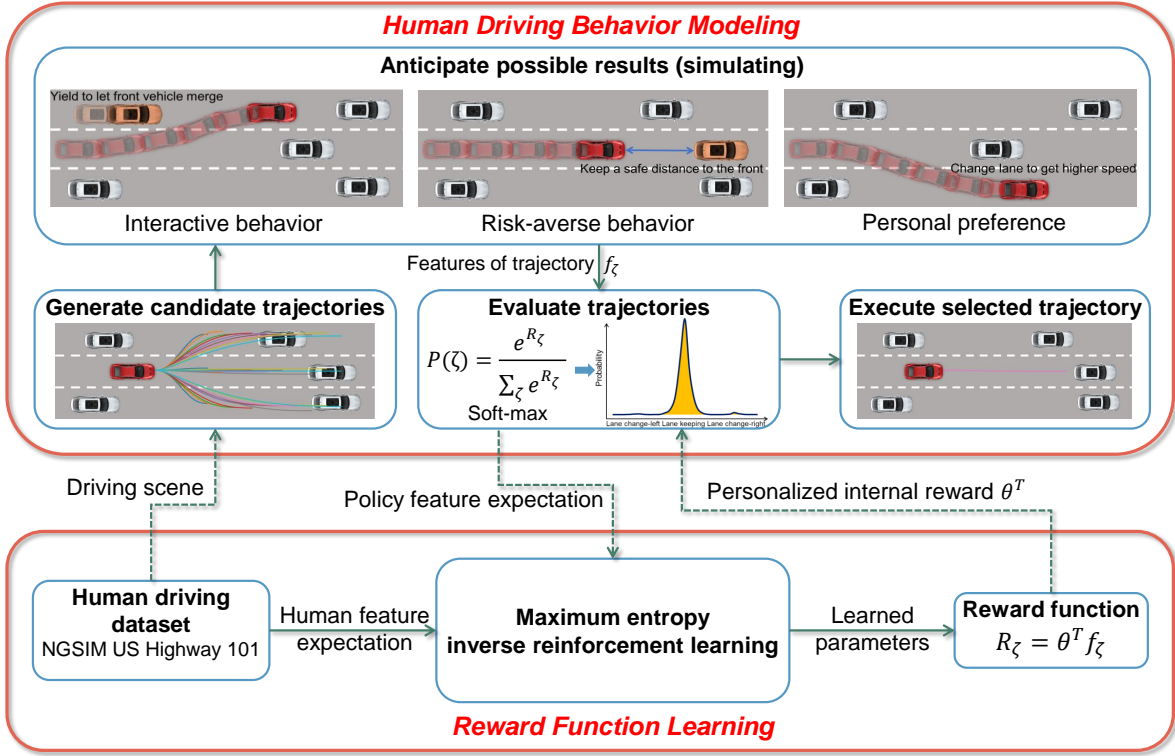


Fig. 1. The framework of internal-reward-function-based human driving behavior modeling using inverse reinforcement learning

to learn the diverse and mixed internal reward functions for multiple human drivers.

### A. Problem statement

Considering a human driver in an arbitrary traffic scene, the state  $s \in \mathcal{S}$  the driver observes consists of the positions of itself and surrounding vehicles, as well as the road context. The action  $a \in \mathcal{A}$  the driver takes is composed of speed and steering controls of the ego vehicle. Assuming that the driver makes a decision on the target state of the vehicle within a finite time horizon  $T$ , a trajectory  $\zeta = [s_1, s_2, \dots, s_T]$  is yielded by organizing the states in each timestep within the decision horizon. Note that the trajectory is a trajectory ensemble including multiple vehicles in the driving scene since we explicitly consider interactions between agents. The human driver evaluate a candidate trajectory according to their internal reward function, and the reward function  $R(s)$  at a specific state  $s$  is defined as the linear combination of features:

$$R(s) = \theta^T \mathbf{f}(s), \quad (1)$$

where  $\theta = [\theta_1, \theta_2, \dots, \theta_K]$  is the weight vector and  $\mathbf{f}(s)$  is the extracted feature vector  $\mathbf{f}(s) = [f_1(s), f_2(s), \dots, f_K(s)]$  that characterizes the state  $s$ . Therefore, the reward of a trajectory  $R_\zeta$  is given as:

$$R_\zeta = \theta^T \mathbf{f}_\zeta = \theta^T \sum_{s \in \zeta} \mathbf{f}(s), \quad (2)$$

where  $\mathbf{f}_\zeta$  denotes the accumulative features along the trajectory  $\zeta$ .

Given the human driving demonstration dataset  $\mathcal{D} = \{\zeta_1, \zeta_2, \dots, \zeta_N\}$  consisting of  $N$  trajectories, the goal of IRL is to infer the reward weights  $\theta$  that can generate a driving policy to match the human demonstration trajectories. We adopt the maximum entropy IRL algorithm described below.

### B. Maximum entropy inverse reinforcement learning

Built on the principle of maximum entropy, maximum entropy IRL assumes a maximum entropy (exponential family) distribution over behaviors, stating that the probability of a trajectory is proportional to the exponential of the reward of that trajectory [11]. Formally,

$$P(\zeta|\theta) = \frac{e^{R_\zeta}}{Z(\theta)} = \frac{e^{\theta^T \mathbf{f}_\zeta}}{Z(\theta)}, \quad (3)$$

where  $Z(\theta) = \int e^{\theta^T \mathbf{f}_\zeta} d\tilde{\zeta}$  is the partition function and  $\tilde{\zeta}$  stands for a feasible trajectory that has the same initial state as  $\zeta$ . This distribution over trajectories produces a stochastic policy, according to which the probability of actions executed from the initial state can be derived.

The averaged log-likelihood  $L(\theta)$  of the demonstration set regarding the reward weights is

$$L(\theta) = \frac{1}{N} \log P(\mathcal{D}|\theta) = \frac{1}{N} \sum_{i=1}^N \log P(\zeta_i|\theta), \quad (4)$$

where  $\mathcal{D} = \{\zeta_i\}_{i=1}^N$  is the trajectory set of human demonstrations.

The goal of maximum entropy IRL is to find the weights  $\theta^*$  that maximizes the likelihood of the human demonstration:

$$\theta^* = \arg \max_{\theta} L(\theta). \quad (5)$$

Although cannot be solved analytically, Equation (5) can be solved using gradient-based optimization. The gradient of the log-likelihood  $L(\theta)$  is the difference of feature expectations between the human trajectories and the generated ones, which is shown as

$$\nabla_{\theta} L(\theta) = \frac{1}{N} \sum_{i=1}^N (\bar{\mathbf{f}}_{\zeta_i} - \tilde{\mathbf{f}}_{\zeta_i}), \quad (6)$$

where  $\bar{\mathbf{f}}_{\zeta_i}$  is the feature vector of the human demonstrated trajectory  $\zeta_i$ , and  $\tilde{\mathbf{f}}_{\zeta_i}$  is the feature expectation of all possible trajectories that share the initial state of  $\zeta_i$ , given as

$$\tilde{\mathbf{f}}_{\zeta_i} = \int P(\tilde{\zeta}_i | \theta) \mathbf{f}_{\tilde{\zeta}_i} d\tilde{\zeta}_i. \quad (7)$$

The problem is that the partition function  $Z(\theta)$  and thus Eq. (7) are intractable for continuous state and action spaces because it requires integrating over the entire class of possible trajectories. However, considering that human driving follows the constraints of traffic rules and the motion of the vehicle, the space of possible trajectories can be reduced to some small subspace. Therefore, we assume that the human driver pre-plans a limited number of trajectories and then select one to follow, which makes it reasonable to approximate the partition function and the feature expectation with multiple generated feasible trajectories. The feature expectation in Eq. (7) can be rewritten as

$$\tilde{\mathbf{f}}_{\zeta_i} \approx \frac{\sum_{j=1}^M e^{\theta^T \mathbf{f}_{\tilde{\zeta}_i^j}}}{\sum_{j=1}^M e^{\theta^T \mathbf{f}_{\tilde{\zeta}_i^j}}} \mathbf{f}_{\tilde{\zeta}_i^j}, \quad (8)$$

where  $\tilde{\zeta}_i^j$  is a generated trajectory,  $\mathbf{f}_{\tilde{\zeta}_i^j}$  is the feature vector of the trajectory, and  $M$  is the number of generated trajectories.

In order to efficiently generate feasible trajectories in a structured environment (e.g., highway), we assume a human driver makes a short-term plan from the current state to an end target and considers the longitudinal and lateral targets respectively. For the longitudinal direction, the driver decides the target speed and for the lateral direction, a tactical decision on lane-changing and lane-keeping is made. Therefore, it is very convenient to use polynomial curves to represent the planned trajectories, which is illustrated below.

### C. Trajectory sampling

We use the Frenet coordinate with reference to the origin and path of the road, to represent the trajectory of a vehicle into the longitudinal and lateral axis. The generated trajectory with regard to longitudinal  $x$  and lateral  $y$  coordinates are quintic polynomial function and quartic polynomial function, respectively, as yielded:

$$\begin{cases} \mathbf{x}(t) = a_0 + a_1 t + a_2 t^2 + a_3 t^3 + a_4 t^4 \\ \mathbf{y}(t) = b_0 + b_1 t + b_2 t^2 + b_3 t^3 + b_4 t^4 + b_5 t^5 \end{cases} \quad (9)$$

Given the initial state of the ego vehicle and the target state, as well as the required time  $T$  to reach the target, the boundary

conditions of the polynomial functions on the longitudinal and lateral axis are:

$$\begin{cases} \mathbf{x}(t=0) = x_s \\ \dot{\mathbf{x}}(t=0) = v_{xs} \\ \ddot{\mathbf{x}}(t=0) = a_{xs} \\ \dot{\mathbf{x}}(t=T) = v_{xe} \\ \ddot{\mathbf{x}}(t=T) = a_{xe} \end{cases}, \begin{cases} \mathbf{y}(t=0) = y_s \\ \dot{\mathbf{y}}(t=0) = v_{ys} \\ \ddot{\mathbf{y}}(t=0) = a_{ys} \\ \mathbf{y}(t=T) = y_e \\ \dot{\mathbf{y}}(t=T) = v_{ye} \\ \ddot{\mathbf{y}}(t=T) = a_{ye} \end{cases} \quad (10)$$

where  $(x_s, v_{xs}, a_{xs}, y_s, v_{ys}, a_{ys})$  is the start state ( $t=0$ ) including position, velocity, and acceleration in the longitudinal and lateral directions;  $(v_{xe}, a_{xe}, y_e, v_{ye}, a_{ye})$  is the target state ( $t=T$ ) without specifying the target longitudinal position.

By solving the boundary equations, the coefficients of the polynomial functions are determined, and thereby a trajectory is generated. The coordinate  $(x_t, y_t)$  on the trajectory at any given time  $t$  ( $t \leq T$ ) can be derived. We can generate multiple trajectories by sampling the target state from the target space  $\Phi = \{v_{xe}, a_{xe}, y_e, v_{ye}, a_{ye}\}$ , which sufficiently covers possible maneuvers. Fig. 2 shows an example of the trajectory generation process, in which only  $v_{xe}$  and  $y_e$  are variable while others are constant to 0. In Fig. 2, the ego vehicle generates multiple candidate trajectories covering the decisions on lane-changing and lane-keeping, as well as the desired longitudinal speed.

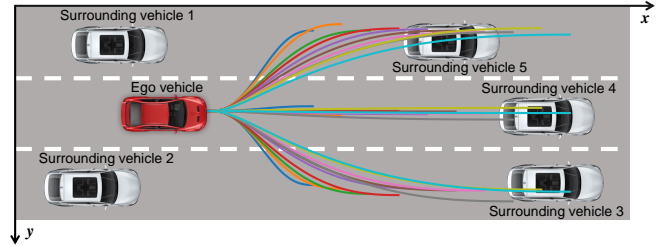


Fig. 2. Trajectory generation process

The next step is to evaluate the reward of each candidate trajectory in a human-like manner. The key component of human driving is interactions with others, which is difficult to estimate with only a static driving dataset. This is because the future trajectories of other traffic participants are highly dependent on the action of the ego human driver, and the human driver's action is dependent on how they value the influence they impose on others. Since the generative trajectory may deviate from the original human behavior in the dataset, an environment model is necessary to help simulate the reactions of other agents to the generative actions. Hence, we build a highly interactive environment in which the vehicles not just follow their original trajectories but react to the actions of the ego vehicle (detailed in Section III-B), so that we can estimate the reward of the generated trajectory considering interaction awareness. The multiple generated trajectories are executed from the current state in the environment model to estimate their accumulative rewards. The underlying assumption is that humans are best-response agents who can anticipate other agents' reactions to their planned actions accurately.

The algorithm of maximum entropy IRL with trajectory sampling is summarized in Algorithm 1.

---

**Algorithm 1:** Maximum entropy inverse reinforcement learning with trajectory sampling
 

---

**Input :** Human demonstrated trajectory dataset  $\mathcal{D} = \{\zeta_i\}_{i=1}^N$ , environment model  $P$ , learning rate  $\alpha$

**Output:** Optimized reward function parameters  $\theta^*$

- 1 Initialize  $\theta \leftarrow \mathbf{0}$ ;
- 2 Initialize buffer  $\mathcal{B} \leftarrow []$ ;
- 3 Compute human feature expectation  $\bar{\mathbf{f}} \leftarrow \frac{1}{N} \sum_{i=1}^N \mathbf{f}_{\zeta_i}$ ;
- 4 **foreach**  $\zeta_i$  in  $\mathcal{D}$  **do**
- 5     Determine the sampling space  $\Phi$  and planning horizon  $T$ ;
- 6     Generate a trajectory set  $\tilde{\mathcal{D}}_i = \{\tilde{\zeta}_i^j\}$  with the same initial state as  $\zeta_i$ ;
- 7     **foreach**  $\tilde{\zeta}_i^j$  in  $\tilde{\mathcal{D}}_i$  **do**
- 8         Rollout the trajectory  $\tilde{\zeta}_i^j$  in the environment model  $P$  and calculate the features of the trajectory  $\mathbf{f}_{\tilde{\zeta}_i^j}$ ;
- 9         Add trajectory and features to buffer  $\mathcal{B} \leftarrow \mathcal{B} \cup \{\tilde{\zeta}_i^j, \mathbf{f}_{\tilde{\zeta}_i^j}\}$ ;
- 10     **end**
- 11 **end**
- 12 **while** not converged **do**
- 13     Calculate the feature expectation with the collected samples from  $\mathcal{B}$
- 14     
$$\tilde{\mathbf{f}} \leftarrow \frac{1}{N} \sum_{i=1}^N \sum_j \frac{\exp(\theta^T \mathbf{f}_{\tilde{\zeta}_i^j})}{\sum_j \exp(\theta^T \mathbf{f}_{\tilde{\zeta}_i^j})} \mathbf{f}_{\tilde{\zeta}_i^j};$$
- 15     Calculate the gradient  $\nabla_{\theta} L(\theta) \leftarrow \bar{\mathbf{f}} - \tilde{\mathbf{f}}$ ;
- 16     Update reward parameters  $\theta \leftarrow \theta + \alpha \nabla_{\theta} L(\theta)$ ;
- 17 **end**
- 18  $\theta^* \leftarrow \theta$

---

### III. EXPERIMENTAL VALIDATION

#### A. Dataset

To validate the proposed method for modeling human driving behavior, we use the Next Generation Simulation (NGSIM) dataset [23] with a segment of data within 7:50 to 8:05 a.m. on the US Highway 101. The recording area is a section of the highway with approximately 640 meters in length and consists of five main lanes and an auxiliary lane, as well as an on-ramp and an off-ramp. The dataset provides the precise location of each vehicle at 10 frames per second within the recording area relative to the local coordinate, resulting in detailed vehicle trajectories. It includes the trajectories of nearly 3000 vehicles and provides rich information on interactions between human drivers, which is necessary for our study to reveal the diverse, personalized, and highly interactive human driving behaviors. The originally collected vehicle trajectories in the dataset are full of observation noise, and thus we use the Savitzky-Golay filter to smooth the original trajectories and obtain the demonstration trajectories for reward learning.

#### B. Interactive environment

The static driving dataset cannot fully reflect the interactive awareness of human drivers that their actions are interdependent on each other. In order to address this issue, we build a simulator that allows for taking control of the target vehicle and playing back the original trajectories of the surrounding vehicles, while the surrounding vehicles can be overridden by IDM models to avoid a potential collision. The simulator serves as an environment model, or in a sense a simulated mental world of human drivers, to anticipate other agents' reactions to the ego movements and help estimate the reward of the generated trajectory. We first construct the road network the same as the recording area on Highway 101 and then spawn vehicles on the road as recorded in the dataset, one of which is targeted as the observation object and maneuvered by a pure-pursuit controller to track the generated trajectory. Other vehicles come after their recorded trajectories and constantly check the gap between themselves and the vehicle in front of them. If the front is the ego vehicle and the gap between them is smaller than the desired gap given by the IDM model, the vehicle is overridden by the IDM model and thus does not follow its original trajectory anymore. This rule also applies to the situation that the front vehicle is one that has been overridden by the IDM model and therefore multiple vehicles can be affected sequentially. Fig. 3 shows some exemplar scenarios where the vehicle painted in green is the ego vehicle, and the vehicles in blue are surrounding vehicles following their original trajectories. The yellow ones are the vehicles that have been affected by the ego vehicle's actions and thus been overridden by the IDM model. Vehicles becoming red indicate that they have collided with others.

#### C. Feature selection

Features are mappings from state to real values which capture important properties of the state. Here, we assume human drivers value the driving state in the following four main aspects.

1) *Travel efficiency*: this feature is designed to reflect the human's desire to reach the destination as fast as possible, which is defined as the absolute difference between the longitudinal speed of the vehicle and the desired speed:

$$f_v(s) = |v_x - v_{des}|, \quad (11)$$

where  $v_{des}$  is the desired speed.

2) *Comfort*: ride comfort is another factor that human drivers prefer, and the metrics to gauge comfort are longitudinal acceleration  $a_x$ , lateral acceleration  $a_y$ , and longitudinal jerk  $j_x$ :

$$\begin{cases} f_{a_x}(s) = |a_x| = |\ddot{x}| \\ f_{a_y}(s) = |a_y| = |\ddot{y}| \\ f_{j_x}(s) = |\dot{a}_x| = |\dddot{x}| \end{cases} \quad (12)$$

where  $x$  and  $y$  are the longitudinal and lateral coordinate, respectively.

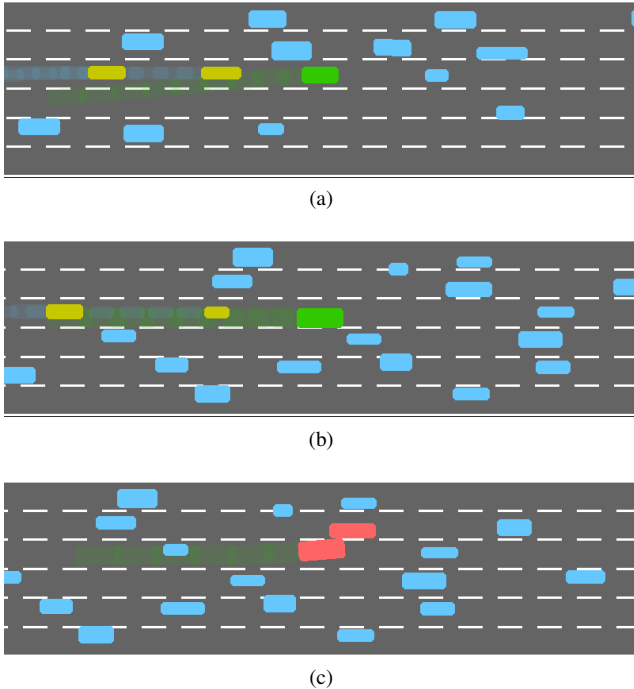


Fig. 3. Illustrations of the interactive environment: (a) the ego vehicle tries to change to the right lane, which makes the affected vehicles decelerate to yield; (b) the ego vehicle runs too slow, which makes the rear vehicles decelerate to avoid a collision; (c) the ego vehicle’s generated trajectory causes a collision and thus this trajectory is deemed infeasible.

3) *Risk aversion*: a human driver tends to keep a safe distance to the surrounding vehicles and this distance varies across different human drivers, which reflects their different levels of sensing risk. We define the risk level to the front vehicle as an exponential function related to the time headway from the ego vehicle to the front vehicle:

$$f_{risk_f}(s) = e^{-\left(\frac{x_f - x_{ego}}{v_{ego}}\right)^2}, \quad (13)$$

where  $x_f$  is the longitudinal position of the nearest front vehicle and  $x_{ego}$  is that of the ego vehicle, and  $v_{ego}$  is the speed of the ego vehicle.

Likewise, the risk level to the rear end is defined as an exponential function related to the time headway from the rear vehicle to the ego vehicle:

$$f_{risk_r}(s) = e^{-\left(\frac{x_{ego} - x_r}{v_r}\right)^2}, \quad (14)$$

where  $x_r$  and  $v_r$  are the longitudinal position and speed of the nearest rear vehicle, respectively.

Note that collision and driving off the road are unacceptable risks and thus these two features have very high costs. We regard the generated trajectories that would cause a collision or go off the road as unfeasible trajectories.

4) *Interaction*: a fundamental property of human driving behavior is that humans are aware of the influence of their actions on the surrounding vehicles and take actions based on their evaluations. More specifically, human drivers care about if their plans impose additional inconvenience to other people (e.g., sharp brake to yield and speed loss). We introduce

the following feature to explicitly evaluate such interaction influence of the generated plans.

$$f_I(s) = \sum_i \max\{v_{i_s} - v_i, 0\}, \quad (15)$$

where  $v_i$  is the speed of the vehicle that has been influenced by the ego vehicle and  $v_{i_s}$  is the initial speed of the vehicle. This feature encodes the speed loss of all the vehicles affected by the ego vehicle’s action.

All the above features are normalized to  $[0, 1]$  to cancel out the influence of their different units and scales.

#### D. Experiment design

1) *Driving behavior analysis*: we utilize the proposed method to analyze the driving behaviors of different human drivers. This follows the personalized modeling assumption that each human driver has different preferences (driving styles), thus having different weights over the reward function, which remain constant with regard to time. Then, the learned reward function is used to determine the probabilities of the candidate trajectories in testing conditions, and to interpret the driving behaviors.

2) *Modeling accuracy*: we show the quantitative results of modeling accuracy by comparing the policy selected trajectories to the ground-truth human driving trajectory. In addition to the personalized modeling method, the general modeling assumption that all drivers share an identical cost function is adopted as a comparison. Two other baseline models are adopted for comparison, which are IDM and MOBIL for longitudinal and lateral movement, respectively, and constant velocity model.

3) *Interaction factors*: we analyze the effects of two interaction factors, including ignoring the ego driver’s awareness of other vehicles’ speed loss and surrounding vehicles not responding to the ego vehicle’s actions. The former aspect is achieved by removing the interaction feature (Eq. (15)), while the latter one is to let the surrounding vehicles stick to their original trajectories instead of being overridden by interactive behaviors.

#### E. Implementation details

For simplicity, the target sampling space is reduced to  $\Phi = \{v_{xe}, y_e\}$ , in which only the longitudinal speed and lateral position are variables and other targets are set as 0. The sampling range of the longitudinal speed is  $[\max\{v - 7, 0\}, v + 7]$  m/s, where  $v$  is the initial speed of the vehicle. The sampling set of the lateral position is  $\{y, y_L, y_R\}$  m, where  $y$  is the initial lateral position, and  $y_L$  and  $y_R$  are the position of the left lane and right lane, respectively, if they are available. We add Gaussian noise  $\epsilon \sim \mathcal{N}(0, 0.3)$  (m) to the target lateral position to emulate the imperfection of human operation. The planning horizon is 5 s and the simulation interval is 0.1 s. The parameters of the IDM model are: desired velocity  $v_0 = v_{current}$  m/s, maximum acceleration  $a_{max} = 5$  m/s<sup>2</sup>, desired time gap  $\tau = 1$  s, comfortable braking deceleration  $b = 3$  m/s<sup>2</sup>, minimum distance  $s_0 = 1$  m.

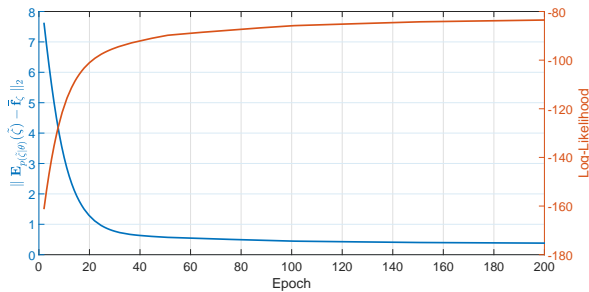
A problem emerges that the longitudinal and lateral jerk of human trajectories and generated trajectories can hardly match because the polynomial curves are smooth while the human driving trajectories are full of noisy movements. Therefore, we process the human driving trajectory to be represented by a polynomial curve given the initial state and end condition of the original trajectory.

To stabilize the training process, Adam optimizer instead of the vanilla gradient descent method is implemented with an learning rate of 0.01.

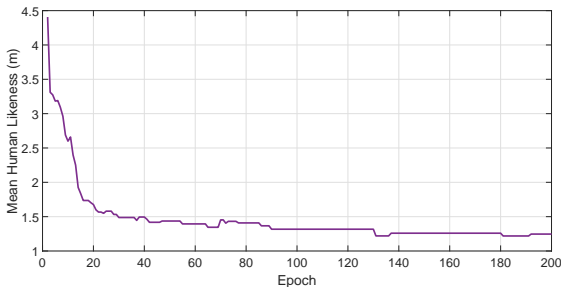
## IV. RESULTS AND DISCUSSIONS

### A. Driving behavior analysis

For a vehicle in the dataset, its whole trajectory in the highway section, which is approximately 50 to 70 seconds in time length, is partitioned into 50 short-term trajectories, each with 5 s length of time. They serve as the training data for reward function learning of a human driver and an example of the training process is shown in Fig. 4, which plots the curves of feature difference between the learned policy and human driver, the log-likelihood of the human demonstrated trajectories, and mean human likeness. The human likeness is a custom metric to gauge the accuracy of the model, i.e., closeness to the ground-truth human driving behavior. Since our model is a generative and probabilistic model, we define the human likeness as the minimal final displacement error of three generated trajectories with the highest probabilities in the distribution over feasible trajectories. Formally, it is defined as  $HL = \min\{\|\hat{\zeta}_i(T) - \zeta_{gt}(T)\|_2\}_{i=1}^3$ , where  $\hat{\zeta}_i$  ( $i = 1, 2, 3$ ) are the selected trajectories with the highest probabilities,  $\zeta_{gt}$  is the ground-truth trajectory by the human driver, and  $T$  is the end of the time horizon. Therefore, smaller human likeness means better modeling accuracy.



(a)



(b)

Fig. 4. Example of the training process: (a) plot of the feature difference and log-likelihood; (b) plot of the mean human likeness.

As seen in Fig. 4a, the log-likelihood of the human demonstrated trajectories gradually increases and converges, recalling that the goal of the maximum entropy IRL is to maximize the likelihood of human demonstrations, and the feature difference between the learned policy and human driver steadily reduces to a small number. This gives rise to the decrease in human likeness as shown in Fig. 4b, which means that the probability of choosing the trajectories close to human driving behavior raises under the learned reward function. Note that the log-likelihood is calculated on the total 50 trajectories of a human driver and the mean human likeness is averaged over these trajectories. The results justify both the effectiveness of the proposed maximum entropy IRL algorithm with trajectory sampling.

Then, we can select human drivers and associated driving trajectories from the dataset and apply the proposed method to infer their individual reward functions, and eventually use the learned reward to interpret the decision-making process of the human drivers. Fig. 5 shows some representative cases of different vehicles from the US-101 highway dataset. The candidate trajectories and their associated probabilities and the ground-truth human driving trajectories are displayed, as well as the trajectories of the surrounding vehicles as the interaction context. Generally, lowering the risk to both the front end and rear end is a critical factor shared by most human drivers, while the other factors (travel speed, ride comfort, and interaction) varies among different human drivers. Fig. 5a shows an overtaking scenario, in which the human driver, as represented by the recovered reward function, views that the travel speed weighs more than the ride comfort (both longitudinally and laterally). If the driver stays in the current lane, a significant efficiency loss is anticipated compared to changing to the right lane. Besides, if the driver chooses to change to the left lane, a notable speed loss can be imposed on the rear vehicle, which is an undesired result since the driver opposes imposing influence on others, given a higher cost weight on the interaction term. This example signifies that our model can accurately predict the lane-changing behavior with a high probability and give a predicted trajectory close to the ground-truth human driving one. For another instance, in Fig. 5b, where the human driver treats the lateral comfort as the main concern, even if changing to the left lane can bring higher efficiency, the driver still keeps the current lane, as predicted by the model with a probability of 65%.

### B. Testing of accuracy

We randomly select 100 vehicles from the dataset, among which 50 vehicles experience lane change while the rest only run lane-keeping, as the target objects. For the personalized modeling assumption that each driver has a unique cost function, the proposed IRL method is applied to infer their individual reward functions. For the general modeling assumption, a total of 150 trajectories from 50 vehicles are used to learn a general cost function shared by all human drivers. The learned cost function is utilized to select the candidate trajectories in the testing conditions and compared with the ground-truth human driving trajectories. Two other

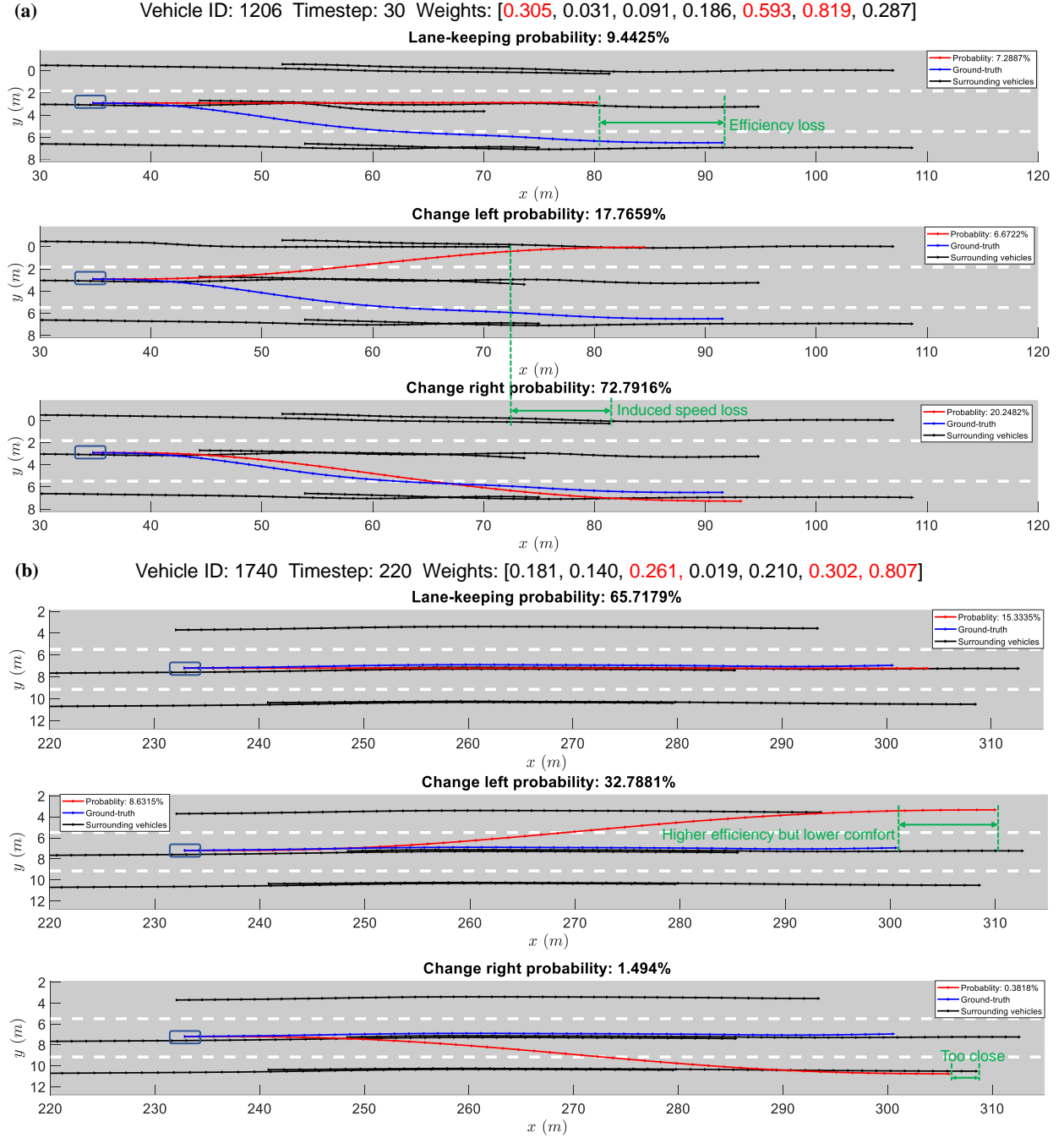


Fig. 5. Driving behavior analysis of some typical cases from the US 101 highway dataset. The weights correspond to the feature vector [travel efficiency, longitudinal acceleration, lateral acceleration, longitudinal jerk, risk to the front, risk to the rear, interaction]. The top-3 important weights are marked in red.

models are selected as comparison baselines, i.e., the IDM and MOBIL models for longitudinal and lateral behaviors and the constant velocity model. For the IDM model, the tuned parameters are: maximum acceleration  $a_{max} = 1.3 \text{ m/s}^2$ , desired time gap  $\tau = 1.2 \text{ s}$ , comfortable braking deceleration  $b = 0.7 \text{ m/s}^2$ , and minimum distance  $s_0 = 1.5 \text{ m}$ ; and the parameters for the MOBIL model are: safe deceleration limitation  $b_{safe} = 2 \text{ m/s}^2$ , politeness factor  $p = 0.01$ , and lane-changing decision threshold  $a_{th} = 0.2 \text{ m/s}^2$ . Two metrics are used to reflect the modeling accuracy, i.e., the mean human likeness on trajectories and intention prediction

accuracy. The intention is divided into two aspects: lane (lane-keeping, left lane changing, and right lane changing) and speed (speed-keeping, acceleration, and deceleration). The ground-truth acceleration intention is defined as the speed change within 5 seconds greater than  $2 \text{ m/s}$ , the deceleration intention as the speed change smaller than  $-2 \text{ m/s}$ , while the rest conditions are deemed as keeping the current speed. We examine the modeling accuracy for individual vehicles, and 30 driving scenes at different timesteps from a vehicle's trajectory in the highway section are randomly selected as the testing conditions. The results of the modeling accuracy of different

models are shown in Fig. 6, in which the boxplots display the summary of the 100 different vehicles.

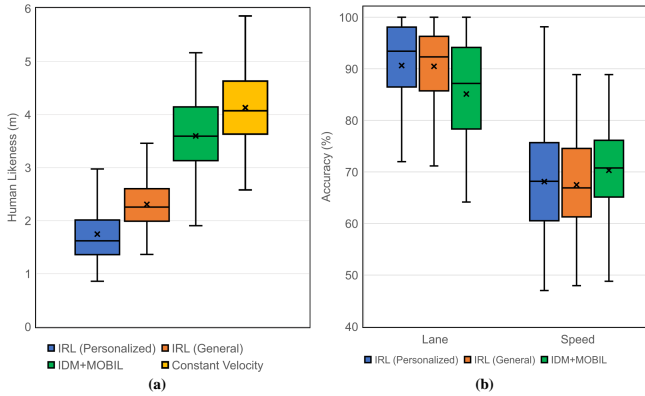


Fig. 6. Comparison of modeling accuracy of different models: (a) human likeness; (b) intention prediction accuracy.

Fig. 6a reveals that personalized modeling is more close to human driving behavior and thus demonstrates smaller errors to the ground-truth trajectories ( $Mean = 1.745 m$ ). A notable reduction in human likeness is found when turning to general modeling ( $Mean = 2.306 m$ ), but it is still significantly better than the IDM and MOBIL models ( $Mean = 3.596 m$ ). Additionally, the difference in human likeness between the personalized modeling and general modeling is statistically significant found by the t-test ( $p < 0.001$ ). The results also imply the interactive models (IRL models and IDM model) outperform the dynamics-based model (constant velocity model). As seen in Fig. 6b, in terms of intention prediction accuracy on speed, all the three models perform at the same level with no significant difference found by the analysis of variance (ANOVA,  $F(2, 100) = 2.3$ ). However, for the intention prediction on selecting lanes, a significant difference is found ( $F(2, 100) = 36.52$ ) and the IRL models get better results than the MOBIL model, since the MOBIL model is hard to tune and cannot fit the diverse preferences of human drivers. These findings suggest that a general cost function can only encode the basic requirements and common preference of human driving behaviors, so that it can be accurate in predicting the high-level intention of the driver but less accurate in predicting the possible trajectories. Only personalized modeling is able to express the diverse human driving preferences and thereby achieves better performance in fitting personalized driving behavior.

### C. Effect of interaction factors

The proposed method gives full considerations to the interaction factors among human drivers, either in taking into account the possible travel efficiency loss on other vehicles caused by the ego vehicle’s movement or in simulating the movement of surrounding vehicles, which makes a dynamic and interactive environment model for the sampling-based IRL algorithm. Here, we investigate how these two interaction factors could affect the modeling accuracy of human driving behaviors in terms of training performance and generalization capability. For the personalized modeling assumption, for

each vehicle, we randomly select 30 trajectories from it to be the training data for the IRL method to learn the cost function, and the rest 20 trajectories are treated as the testing conditions, where the learned cost function is used to select the candidate trajectories. This procedure applies to the same 100 target vehicles and the results are shown in Table I. The metric human likeness is averaged first by the trajectories of a vehicle and then by different vehicles, and the log-likelihood is averaged by vehicles.

TABLE I  
COMPARISON OF TRAINING AND TESTING PERFORMANCE FOR PERSONALIZED MODELING WITH REGARD TO INTERACTION FACTORS

Method	Human likeness (training) [m]	Log-likelihood (training)	Human likeness (testing) [m]	Intention accuracy (testing) [%]
Proposed	1.494	-52.821	<b>1.816</b>	<b>90.28</b>
W/o interaction awareness	1.519	-54.697	1.899	89.91
W/o reactive response	<b>1.433</b>	<b>-51.361</b>	1.876	90.03

It is apparent from Table I that canceling the interaction awareness or the induced travel efficiency loss to other vehicles in the cost function would impair the modeling accuracy, which suggests that the interaction or courtesy factor is of importance in modeling naturalistic human driving behaviors. Another finding is that although not simulating the reactive behaviors of surrounding vehicles may produce better training performance in terms of both human likeness and likelihood, its generalization ability is compromised and testing performance is worse than the proposed method. The issue possibly is caused by the biased estimation of the partition function. For the sampling-based IRL method, generating accurate and possible samples that agree with the realistic human behaviors is key to approximate the partition function. Using the static dataset where all other vehicles go along their fixed paths can make some of the sampled trajectories less likely since these trajectories could cause a crash or become too risky. However, those trajectories are still possible in the real world setting because other drivers can adapt to the ego vehicle’s actions and therefore the stochasticity of human driving behavior is ignored. This could remove or underestimate some sampled trajectories when approximating the partition function, and thus bias the estimation to fit the training data and consequently leading to compromised generalization ability. Therefore, it is reasonable to simulate other vehicles’ response to the sampled trajectories in order to approximate the partition function and learn the parameters of the cost function more accurately.

For the general modeling assumption, a total of 150 trajectories from 50 vehicles are selected as training data to learn a general cost function and then the learned cost function is utilized to select the candidate trajectories of the other 50 vehicles, each with 30 ground-truth driving trajectories. The human likeness and log-likelihood of the training and testing processes are displayed in Table II. Note that the log-likelihood of the testing process is calculated under the learned general cost function and averaged over all testing trajectories.

The findings in Table II are consistent with the findings in Table I, suggesting that ignoring interaction awareness would lower the modeling accuracy and likelihood of human

TABLE II  
COMPARISON OF TRAINING AND TESTING PERFORMANCE FOR GENERAL MODELING WITH REGARD TO INTERACTION FACTOR

Method	Human likeness (training) [m]	Log-likelihood (training)	Human likeness (testing) [m]	Log-likelihood (testing)
Proposed	1.953	-382.711	<b>2.325</b>	<b>-76.952</b>
W/o interaction awareness	1.970	-383.783	2.403	-78.353
W/o reactive response	<b>1.896</b>	<b>-364.164</b>	2.391	-77.958

demonstrations both in training and testing, and not simulating the responses of other vehicles could produce better training performance but undermine the generalization capability.

#### D. Discussions

The application of the proposed human driving behavior modeling method is primarily on the planning and decision-making module of an AV for personalized driving experiences. It is very promising to learn a personalized cost function from naturalistic human driving data offline and integrate the learned cost function into the trajectory planning module, eventually achieving personalized driving experience. Another application is to predict the motion of surrounding vehicles. The cost functions of other vehicles can be inferred online through an offline dataset containing a distribution of cost functions for different driving styles [24] or even acquired via vehicle-to-vehicle communications. Due to the mutual influence of agents, the trajectories of all interacting vehicles should be predicted. This would significantly increase the computation time, but the prediction process can be accelerated by reducing the sampling space or the number of target vehicles and paralleling the sampling process.

Several limitations need to be acknowledged. One is that the model cannot address the irrational decisions that could be made by human drivers. Besides, the assumption of a linear reward function with time-invariant weights may not be held and the handcrafted features cannot fully represent the factors involved in human driving behaviors. The trajectory sampling method can be also improved to address more complicated driving behaviors by, for example, segmenting the 5-second planning horizon into five 1-second intervals and sampling a target state for each interval. Therefore, future works may focus on using a neural network that maps from raw states to reward value to parameterize the reward function so as to improve the expression ability of the model, as well as refining the trajectory sampling method to achieve more accurate estimation of the partition function.

#### V. CONCLUSIONS

In this study, we propose a human driving modeling approach based on internal reward function and a sampling-based IRL method for learning personalized reward functions among human drivers in the highway driving scenario. A polynomial trajectory sampler is used to generate the candidate trajectories covering the high-level decisions (lane-changing and lane-keeping) and the desired speed, while the generated trajectories are used to approximate the partition function in the maximum entropy IRL framework. The interaction factors are fully

considered, including simulating the responses of surrounding vehicles to the agent's behavior and incorporating the travel efficiency loss of other vehicles into the driver's internal reward function. We apply the method to learn the reward functions of different human drivers in the NGSIM dataset and interpret their driving decisions with the learned reward function. The quantitative results on 100 vehicles show that the personalized modeling method significantly outperforms the general modeling method in terms of the human likeness, as well as the IDM+MOBIL model and constant velocity model. In terms of intention prediction, the models deliver performance at the same level. Moreover, without simulating the response actions of the vehicles influenced by the ego vehicle's generated trajectory when learning the reward function could produce better training results but compromise the generalization ability. Besides, without interaction awareness (the ego vehicle's action imposing efficiency loss on other vehicles) could also lower the modeling accuracy.

#### REFERENCES

- [1] L. Li, K. Ota, and M. Dong, "Humanlike driving: Empirical decision-making system for autonomous vehicles," *IEEE Transactions on Vehicular Technology*, vol. 67, no. 8, pp. 6814–6823, 2018.
- [2] C. Basu, Q. Yang, D. Hungerman, M. Sinahal, and A. D. Drahan, "Do you want your autonomous car to drive like you?" in *2017 12th ACM/IEEE International Conference on Human-Robot Interaction (HRI)*. IEEE, 2017, pp. 417–425.
- [3] K. Brown, K. Driggs-Campbell, and M. J. Kochenderfer, "Modeling and prediction of human driver behavior: A survey," *arXiv preprint arXiv:2006.08832*, 2020.
- [4] M. Treiber, A. Hennecke, and D. Helbing, "Congested traffic states in empirical observations and microscopic simulations," *Physical review E*, vol. 62, no. 2, p. 1805, 2000.
- [5] A. Kesting, M. Treiber, and D. Helbing, "General lane-changing model MOBIL for car-following models," *Transportation Research Record*, vol. 1999, no. 1, pp. 86–94, 2007.
- [6] Y. Xing, C. Lv, and D. Cao, "Personalized vehicle trajectory prediction based on joint time-series modeling for connected vehicles," *IEEE Transactions on Vehicular Technology*, vol. 69, no. 2, pp. 1341–1352, 2020.
- [7] X. Mo, Y. Xing, and C. Lv, "Interaction-aware trajectory prediction of connected vehicles using CNN-LSTM networks," *arXiv preprint arXiv:2005.12134*, 2020.
- [8] F. Diehl, T. Brunner, M. T. Le, and A. Knoll, "Graph neural networks for modelling traffic participant interaction," in *2019 IEEE Intelligent Vehicles Symposium (IV)*. IEEE, 2019, pp. 695–701.
- [9] L. Sun, W. Zhan, Y. Hu, and M. Tomizuka, "Interpretable modelling of driving behaviors in interactive driving scenarios based on cumulative prospect theory," in *2019 IEEE Intelligent Transportation Systems Conference (ITSC)*. IEEE, 2019, pp. 4329–4335.
- [10] D. S. González, J. S. Dibangoye, and C. Laugier, "High-speed highway scene prediction based on driver models learned from demonstrations," in *2016 IEEE 19th International Conference on Intelligent Transportation Systems (ITSC)*. IEEE, 2016, pp. 149–155.
- [11] B. D. Ziebart, A. L. Maas, J. A. Bagnell, and A. K. Dey, "Maximum entropy inverse reinforcement learning," in *Aaai*, vol. 8. Chicago, IL, USA, 2008, pp. 1433–1438.
- [12] L. Sun, W. Zhan, and M. Tomizuka, "Probabilistic prediction of interactive driving behavior via hierarchical inverse reinforcement learning," in *2018 21st International Conference on Intelligent Transportation Systems (ITSC)*. IEEE, 2018, pp. 2111–2117.
- [13] Y. Hu, L. Sun, and M. Tomizuka, "Generic prediction architecture considering both rational and irrational driving behaviors," in *2019 IEEE Intelligent Transportation Systems Conference (ITSC)*. IEEE, 2019, pp. 3539–3546.
- [14] M. Kuderer, S. Gulati, and W. Burgard, "Learning driving styles for autonomous vehicles from demonstration," in *2015 IEEE International Conference on Robotics and Automation (ICRA)*. IEEE, 2015, pp. 2641–2646.

- [15] Y. Xu, J. Xie, T. Zhao, C. Baker, Y. Zhao, and Y. N. Wu, "Energy-based continuous inverse optimal control," *arXiv preprint arXiv:1904.05453*, 2019.
- [16] Z. Wu, L. Sun, W. Zhan, C. Yang, and M. Tomizuka, "Efficient sampling-based maximum entropy inverse reinforcement learning with application to autonomous driving," *IEEE Robotics and Automation Letters*, vol. 5, no. 4, pp. 5355–5362, 2020.
- [17] S. Levine and V. Koltun, "Continuous inverse optimal control with locally optimal examples," in *Proceedings of the 29th International Conference on International Conference on Machine Learning*, 2012, pp. 475–482.
- [18] D. S. González, O. Erkent, V. Romero-Cano, J. Dibangoye, and C. Laugier, "Modeling driver behavior from demonstrations in dynamic environments using spatiotemporal lattices," in *2018 IEEE International Conference on Robotics and Automation (ICRA)*. IEEE, 2018, pp. 1–7.
- [19] S. Rosbach, V. James, S. Großjohann, S. Homoceanu, and S. Roth, "Driving with style: Inverse reinforcement learning in general-purpose planning for automated driving," *arXiv preprint arXiv:1905.00229*, 2019.
- [20] X. He, D. Xu, H. Zhao, M. Moze, F. Aioun, and F. Guillemand, "A human-like trajectory planning method by learning from naturalistic driving data," in *2018 IEEE Intelligent Vehicles Symposium (IV)*. IEEE, 2018, pp. 339–346.
- [21] L. Sun, W. Zhan, M. Tomizuka, and A. D. Dragan, "Courteous autonomous cars," in *2018 IEEE/RSJ International Conference on Intelligent Robots and Systems (IROS)*. IEEE, 2018, pp. 663–670.
- [22] W. Schwarting, A. Pierson, J. Alonso-Mora, S. Karaman, and D. Rus, "Social behavior for autonomous vehicles," *Proceedings of the National Academy of Sciences*, vol. 116, no. 50, pp. 24 972–24 978, 2019.
- [23] V. Alexiadis, J. Colyar, J. Halkias, R. Hranac, and G. McHale, "The next generation simulation program," *Institute of Transportation Engineers. ITE Journal*, vol. 74, no. 8, p. 22, 2004.
- [24] L. Sun, Z. Wu, H. Ma, and M. Tomizuka, "Expressing diverse human driving behavior with probabilistic rewards and online inference," *arXiv preprint arXiv:2008.08812*, 2020.